2023 CCM & IMEKO TC16 7th International Conference on Pressure and Vacuum Metrology
IMEKO TC-16 2023
Washington DC, U.S.A., May 15-19, 2023

Negative gauge pressure calibration methods using a PACE CM3 pressure controller

Tim Sparkes, Stefan Berdej, Christopher Roberts, Neculai Moisoi

Druck Ltd, a Baker Hughes business, Fir Tree Lane, Groby, Leicester, LE6 0FH, United Kingdom, Email: neculai.moisoi@bakerhughes.com

Abstract - The development of pressure controllers has seen a great focus and their technical characteristics have improved over the last few decades, specifically in terms of their metrological capabilities. This advancement now makes them a suitable candidate to measure negative gauge pressure, either directly or in conjunction with other devices such as pressure balances. The Druck PACE in conjunction with CM3 (control module) has demonstrated performance characteristics in line with those required to complete negative gauge pressure calibrations. Three different calibration methods were developed within the Druck Ltd laboratory, from which two of them used a 200 kPa absolute pressure CM3, containing TERPS© (Trench Etched Resonant Pressure Sensor). The unit under test was a PACE1000 indicator built with a piezoresistive sensors with a pressure range from -100 to 100 kPa. The expanded uncertainty was evaluated for each method, as well as identifying the advantages and shortcomings of each method. As the calibrations were performed for gauge mode (not differential), the calibration range was -950 to -50 hPa.

I. TERPS© TECHNOLOGY

The TERPS© technology was developed from the beginning to be a high performance pressure sensor, with unique metrological characteristics, which were vital in the experiments presented below. From the design to construction, each stage was optimized to eliminate unwanted effects and ensure a monotonic signal was obtained across the required pressure range.

TERPS© construction has a pressure sensing diaphragm connected to a mechanical structure that is induced to resonate at its natural frequency. When pressure is applied to the diaphragm the resonating structure is stretched resulting in a change to the frequency of the resonator (Fig. 1.). Silicon resonant pressure sensors have high resolution and sensitivity, are very stable and exhibit low hysteresis resulting in overall excellent performance.

Using this technology pressure sensors with ranges from barometric to 21.1 MPa may be produced with higher pressures currently in development. At a silicon manufacturing level, some of the most important steps taken to achieve the TERPS© performance are: using Silicon-on-Insulator (SOI) to control thickness and mass of resonating structure, optimizing deep reactive ion etching (DRIE) process to create well defined patterned structures for dynamic mass and force balance and using silicon fusion bonding (SFB), which eliminates the thermal mismatch when different materials are used.

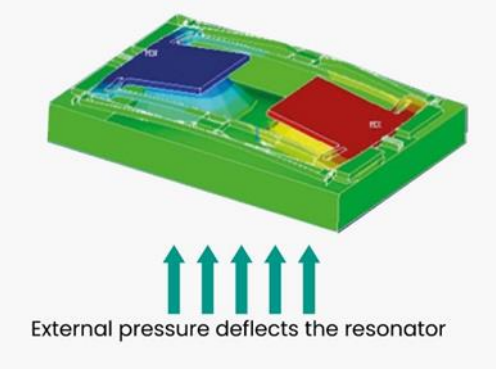

Fig. 1. FEA showing the deflection of mesas (pillars) under pressure.

Another key element of the design was to design and optimize a lateral resonator so the loss of energy to the diaphragm is minimised and the excitation of unwanted modes is suppressed. This design feature has also the added

advantage of having a very low energy loss, which results in a quality factor (or Q-factor) above 40,000. Such a high Q-factor allows the frequency of the resonator to be measured to a high resolution and indicates a low coupling to supports resulting in improved long-term stability.
Packaging stresses are minimized by isolating the silicon chip from the package with the use of an anodically bonded glass support & by low stress chip packaging techniques (Fig. 2.). All these factors combine, resulting in extremely stable performance and low hysteresis.

Fig. 2. Silicon die packaged in a glass-to-metal seal

The frequency output from a resonant sensor can be measured with very high precision and the digital circuitry, unlike analogue circuitry, is immune to drift and external noise & interference.
Overall, each step in design and manufacturing were made to enable TERPS© to achieve precision (Linearity, Hysteresis, Repeatability and Thermal Effects) better than 10 ppm FS and expanded uncertainties ~ 20 ppm (mix of reading and FS contributions).

II. CALIBRATION METHODS DESCRIPTION

A. First Method

The first method (Method A) was a direct method. The CM3 was used to apply the pressure to the PACE1000 indicator (UUT) [1], while using a barometer to record the atmospheric pressure variation (Fig. 3.). To reduce the impact of the atmospheric pressure changes, an A-B-A method was used to collect the data, where A is the barometer reading and B is unit under test, while maintaining the applied pressure constant (within the repeatability of the CM3 controller).

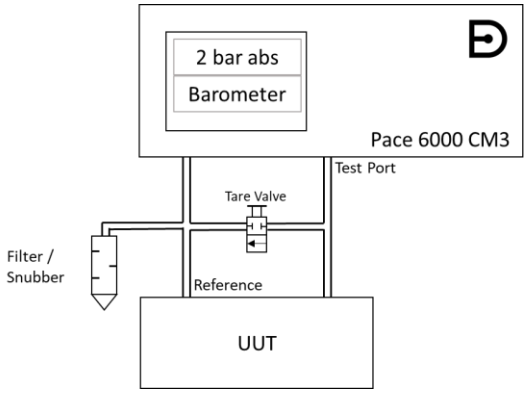

Fig. 3. Method A Test Setup

In the equation below, P_n represent the evaluated negative pressure, while P_{abs} is the pressure applied by the PACE controller and P_b is the measured barometric pressure. The "zero" index denotes the initial values used to eliminate the systematic offset between the PACE and the barometer.

The control stability of the controller is required to be ~1 ppm or better, which is achievable with a well set-up controller. There will always be a requirement to allow the controller to stabilize and dissipate the adiabatic thermals present within the system.

$$\boldsymbol{P_n = P_{abs} - P_b - P_{abs0} + P_{b0}} \qquad (1)$$

Rapid variations in atmospheric pressure were reduced by using a filter or snubber on the reference pipework common to both the UUT and the PACE calibrator. Further enhancement may be made by introducing a volume into the reference system, effectively increasing the effect of the snubbers restriction in flow to stabilize the reference port. This method is, by its design, reliant of the atmospheric pressure and therefore low atmospheric pressures will limit the range of measurement possible in the -ve gauge range.

B. Second Method

The second method (Method B) used the CM3 controller to apply a negative pressure to the bell jar of a pressure balance [2], while the positive port is open to the atmospheric pressure (Fig. 4.). The applied pressure from the pressure balance was calculated at each measurement point, while minimizing the influencing factors effects. [1].

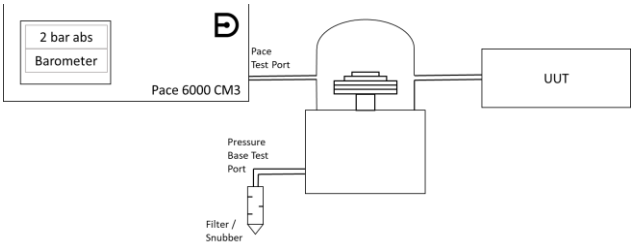

Fig. 4 Method B Test Setup

$$\boldsymbol{P_{neg}} = -\frac{\sum_i [\, m_i\left(1-\frac{\rho_a}{\rho_m}\right).g]}{A_0[1+(\propto_p+\propto_c).(t-t_{ref}).[1+\lambda.P]} + \left(\rho_f - \rho_a\right).g.\Delta h \quad (2)$$

where:

m_i: Mass of the piston and the weights

g: Acceleration due to gravity in the laboratory

A_0: Effective area of piston-cylinder assembly at zero pressure and temperature t_{ref}

α_p: Linear thermal expansion coefficient of the piston

α_c: Linear thermal expansion coefficient of the cylinder

t: Temperature of piston-cylinder assembly

t_{ref}: Reference temperature of piston-cylinder assembly

λ: Deformation coefficient of piston-cylinder assembly

P: Nominal value of measured pressure

μ: Residual pressure in the bell jar

ρ_f: Density of the fluid at the measured pressure

Δh: Height difference between the pressure balance and the unit under test

ρ_a: Density of the air in the bell jar

ρ_m: Density of the pressure balance weights

The unit under test was connected opposite the controller, through the bell jar, which helped to reduce the pressure variation observed during the measurements. The PACE controller was used in 'nudge' mode to manually adjust the float of the piston. Ultimately 'nudge' values of less than 0.1 Pa were used to achieve a constant float position. It is intended that, with the addition of an automatic float height measurement and suitable software, this operation could be performed automatically, and the fall rate of the piston optimized. One difficulty observed during this calibration was that an increase or decrease of atmospheric pressure caused the reference pressure (positive port) to change and the pressure balance equilibrium point was subsequently affected. This approach requires the atmospheric pressure to be relatively stable at each calibration point and an improvement to the method is described below.

C. Third Method

The third method (Method C) used an inverted piston-cylinder assembly of a pressure balance [2] with the unit under test directly connected to its port (Fig. 5.). This method is a well-established method in the Druck UKAS laboratory, and it was used as a comparison with the first two methods. The control pack is made of a manual system of valves, which control the pressure/vacuum to achieve the equilibrium for pressure balance.

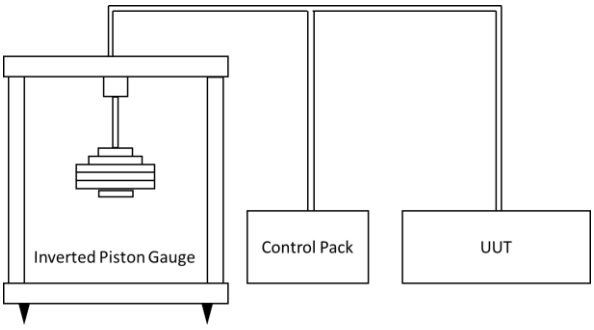

Fig. 5. Method C Test Setup

The results were analyzed to understand the current expanded uncertainty capability given by these methods as well as the potential to develop these methods further to allow users the possibility to perform easier calibrations with high accuracy and relative low cost.

III. UNCERTAINTY EVALUATION

For method A, the evaluation of the expanded uncertainty has shown there are four main factors, affecting the results: the calibration of the CM3, barometric pressure changes, CM3 repeatability and CM3 long term span drift (Table 1.).

Table 1. CM3 & Barometer Uncertainty Budget [4]

Source of uncertainty/unit	Symbol	Value	Uncertainty	Probability distribution	Divisor	Sensitivity coefficients	u_i /Pa
CM3 Standard Calibration Uncertainty [Pa]	Pc	95000.00	1.6E+00	Normal	2	1.00E+00	0.818
CM3 Repeatability [ppm FS]	R	2.00	4.0E-01	Normal	1	1.00E+00	0.400
CM3 long term span drift [ppm FS]	Pd	5.00	4.8E-01	Uniform	√3	1.00E+00	0.274
Fluid head height [m]	H	0.01	2.0E-03	Uniform	√3	1.06E+01	0.012
Working Fluid Density [kg/m³]	ρf	1.08	1.1E-01	Uniform	√3	9.81E-02	0.006
Acceleration due by gravity [m/s²]	g	9.81291	3.0E-05	Uniform	√3	1.08E-02	0.000
Barometer resolution [Pa]	Rb	0.10	1.0E-01	Uniform	√3	1.00E+00	0.058
Barometer pressure change[Pa]	Cb	100.00	1.0E+00	Uniform	√3	1.00E+00	0.577
	Combined standard uncertainty			Normal			1.114
	Expanded uncertainty (k=2)			Normal			2.227

The calibration uncertainty is dependent on the capability of the NMIs used for calibration, but both, the uncertainty sources for the repeatability of the CM3 and its span drift, can be further improved as the TERPS© technology

matures even further. The barometric pressure change was caused mainly by the atmospheric pressure changing relatively rapidly during our experiments and on a meteorologically more stable day this can be also reduced further.

However, the noise due to atmospheric pressure changes was minimized by using a filter on the barometer input, which reduces the faster frequency changes.

The calibration expanded uncertainty was evaluated for the calibration points in the -950 to -50 hPa range and its value is U = 1.4 Pa + 7 ppm of reading.

Method B includes many factors (Table 2.) influencing the expanded uncertainty of the calibrations, due to the use of the pressure balance, but through careful considerations, most of the influences have been minimized. The main factors were due to the pressure balance calibration: effective area and the mass of the weights and the density of the masses, as it wasn't directly measured but evaluated from manufacturer data.

Table 2. Pressure Balance -Bell Jar Method Uncertainty Budget [4]

Uncertainty budget for Negative Gauge Calibration using a Pressure Balance Bell Jar Method							
Source of uncertainty/unit	Symbol	Value	Uncertainty	Probability distribution	Divisor	Sensitivity coefficients	u_i /Pa
Repeatability / ppm of RDG	R	1.00	1.0E-01	Normal	1	1	5.00E-02
Effective Area of the DWT/ m²	A0	0.00	8.0E-09	Normal	2	3.00E+08	1.20E+00
Drift of above area / m²	dA0	0.00	4.7E-10	Rectangular	√3	3.00E+08	8.08E-02
Mass on the DWT /kg	m	3.40	1.4E-05	Normal	2	2.94E+04	2.00E-01
Drift of above mass/ kg	dm	3.40	6.8E-06	Rectangular	√3	2.94E+04	1.15E-01
Acceleration due by gravity/ m/s²	g	9.81	3.0E-05	Normal	2	1.02E+04	1.53E-01
Air Density/ kg/m³	ρ_a	1.20	1.2E-01	Rectangular	√3	1.13E-03	7.85E-05
Mass Density /kg/m³	ρ_m	7800.00	2.0E+02	Rectangular	√3	1.97E-03	2.28E-01
Fluid head / m	h	0.01	2.0E-03	Rectangular	√3	1.18E+01	1.36E-02
Working Fluid Density /kg/m³	ρ_f	1.13	1.1E-01	Rectangular	√3	9.81E-02	6.41E-03
Pressure dependent term / 1/Pa	λ	0.00	0.0E+00	Normal	2	1.00E+10	0.00E+00
Nominal pressure / Pa	p_n	100000.00	1.5E+01	Rectangular	√3	0.00E+00	0.00E+00
Temperature coefficient / 1/°C	α	0.00	5.0E-07	Rectangular	√3	1.56E+00	4.50E-07
Temperature Measurement	t	0.20	5.0E-02	Rectangular	√3	3.12E-01	9.01E-03
Tilt of the pcu /Pa	Δα	0.00	1.5E-01	Rectangular	√3	1.00E+00	8.66E-02
Angular velocity of the piston /Pa	Δω	0.00	1.0E-01	Rectangular	√3	1.00E+00	5.77E-02
Piston taper /Pa	Δτ	0.00	2.0E-01	Rectangular	√3	1.00E+00	1.15E-01
DWT sensitivity /Pa	Δσ	0.00	2.0E-01	Rectangular	√3	1.00E+00	1.15E-01
	Combined standard uncertainty			Normal			1.27E+00
	Expanded uncertainty (k=2)			Normal			2.54E+00

The calibration expanded uncertainty estimated for this method was U = 0.13 Pa + 24 ppm of reading.

Method C uncertainty budget is very similar with method A, but the effective area uncertainty of the calibration standard increased since the pressure balance used was calibrated only in positive mode. The overall expanded uncertainty was estimated to be U = 0.15 Pa + 27 ppm of reading.

IV CALIBRATION METHODS COMPARISON

The calibration results from each Method outlined above were compared, not only graphically but using the EN factor to understand the compatibility of the results. Please note that all the calibration methods used the same calibration points. On the below graph (Fig. 6.) they are offset so that the measurement errors and their associated expanded uncertainties are visible.

Fig. 6. Calibration Methods Comparison

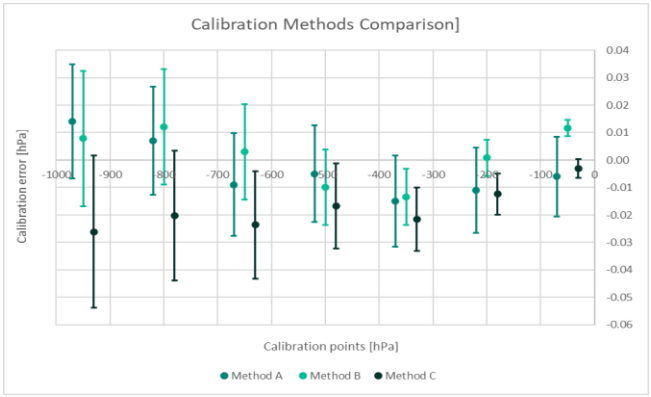

The EN factor was evaluated using the equation:

$$EN = \frac{|P_j - P_i|}{\sqrt{U(P_j)^2 + U(P_i)^2}} \qquad (3)$$

Where i & j indexes represent the method used (A, B, C) and the p are the evaluated gauge pressures with their associated expanded uncertainty U.

The methods A & B results have shown to agree with each other with the EN factor ranging from 0.2 to 0.7, except the highest (-50 hPa) pressure where the value is 1.2. Method C and Method A have agreed with each other except at the lowest point, where EN=1.2. The methods B and C have shown bigger discrepancy with EN factor values ranging between 0.1 to 3.9. Investigating further, a systematic error seems to affect the effective area of the pressure balance used for the method C, which explains the relative larger deviations of this method from the other two.

V.FUTURE DEVELOPMENTS AND CONCLUSIONS

Method A may now be modified with the release of new PACE software which allows the auto zero of the precision reference transducer against the high-performance barometer effectively automating the manual zero and Pb term. This puts the system into pseudo-gauge mode providing a simplified and automatable operating method.

With Method B, the main issue was the time taken to achieve the stable conditions during measurement and ensure the correct measurements were taken. Therefore, this method may be enhanced by utilizing a differential method through the twin controller option on the PACE. Controller 2 provides the 100 kPa absolute reference pressure while controller 1 provides the test pressure (Fig. 7.). Floating of the deadweight would remain the same as previous, variance in atmospheric pressure is obviated and the full range of -ve calibration may be achieved. The method proposed solves another issue with negative gauge calibration, when it comes to working with lower atmospheric pressure, which affect the lowest calibration point measured. This method allows the reference pressure to be kept to a desired artificial atmospheric pressure (e.q. 100 kPa).

Fig. 7. Revised Method B Test Setup

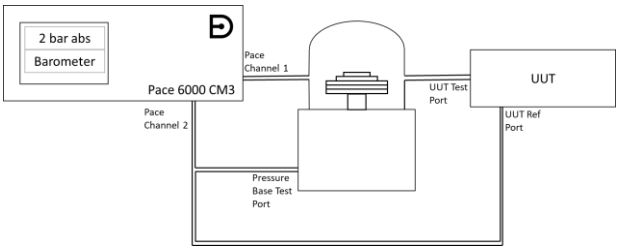

Method C is one of the more commonly used methods for negative gauge calibrations, but it is not always straight forward, as the pressure balance is calibrated with only positive pressure and therefore the distortion (pressure dependent coefficient) influence is therefore not fully understood when using it in negative mode [2]. To use this method effectively, a bespoke system must be setup to accommodate existing pressure balances.

Overall, all three methods were found to be suitable for negative gauge calibration in secondary laboratories with the right precautions in place. The main sources of uncertainties come from the calibration of the standards used. Method A is simpler and faster to use however and provides similar uncertainty results as Method B. Due to its simplicity, the process can be completed successfully irrespective of the skill level of the calibration technicians.

REFFERENCES

[1] Druck Ltd 2008, Druck PACE5000 / 6000 Pressure Automated Calibration Equipment Instruction Manual, K0443 Release d

[2] Djilali Bentouati, Yasin Durgut, Pierre Otal, Mark Plimmer, Dominik Pražák, Wladimir Sabuga, Sven Ehlers and Ekrem Sınır, Calibration methods for negative gauge pressure down to −100 kPa, Meas. Sci. Technol. 29 (2018)

[3] Dadson R, Lewis S L and Peggs G N, 1982 The Pressure Balance: Theory and Practice (London)

[4] ISO/IEC Guide 98-3:2008, Guide to the expression of uncertainty in measurement (GUM)